Wireless Pers Commun (2018) 99:953–964
https://doi.org/10.1007/s11277-017-5160-9

Hybrid Analog and Digital Precoding Based on Adaptive Method in P2P Massive MIMO

Yongpan Feng[1] · **Suk Chan Kim**[1]

Published online: 5 February 2018

Abstract To achieve a far higher capacity in massive multi-input multi-output, the hybrid analog and digital precoding has been studied recently. In this paper, we consider the downlink single user communication system and propose an efficient matrix adaptive gradient descent algorithm to design the radio frequency precoder and combiner, and use the singular value decomposition method to obtain the digital precoder and combiner. Simulation results show that the proposed method can approach the performance of the conventional full digital precoding with a fast convergence rate.

Keywords Massive MIMO · Large-scale antenna · Hybrid precoding · RF precoder · Matrix adaptive

1 Introduction

The upcoming 5G networks aim at carrying out a far higher capacity by 2020 [2]. To achieve this objective, the conception of massive multi-input multi-output (MIMO) has been proposed recently years [5, 7]. Conventional MIMO precoding requires a dedicated baseband and radio frequency (RF) chain for each antenna element, which is prohibitive cost and power consumption for massive MIMO.

To solve this problem, the hybrid analog and digital precoding is proposed [1, 3, 4, 8–10]. Reference [4] proposed successive interference cancelation (SIC) based hybrid precoding aimed at improving energy efficiency. Reference [10] proposed an alternative iterative coordinate descent algorithm. Although it approached the performance of fully digital precoding, its computational complexity was very high. References

✉ Suk Chan Kim
sckim@pusan.ac.kr

Yongpan Feng
fypan@pusan.ac.kr

[1] Department of Electronics Engineering, Pusan National University, Busan, Korea

[1, 3, 8, 9] developed several iterative algorithms based on partial channel knowledge and the matching pursuit method (MP). However, these algorithms were restricted to the Saleh-Valenzuela channel model.

In this paper, an efficient matrix adaptive gradient descent algorithm method has been proposed to design the RF precoder. Numerical simulations show that the proposed algorithm closely matches the performance of the fully digital precoding, and has relatively low computational complexity.

2 System Model

Consider a narrowband downlink P2P MIMO system in which the BS with N antennas and the user (i.e., fixed or mobile base station) with M antennas. To void the fully digital precoding, we consider a two-stage hybrid digital and analog precoding architecture on both the BS and user sides as shown in Fig. 1.

On the BS side, S data streams are inputted into a baseband precoder $\mathbf{W} \in \mathbb{C}^{K_t \times S}$ and enters into a RF precoder $\mathbf{V} \in \mathbb{C}^{N \times K_t}$ (in which the modulus of each element is a constant, i.e., $1/\sqrt{N}$) after go through K_t RF chains, and then those precessed signals are propagated into the wireless channel $\mathbf{H} \in \mathbb{C}^{M \times N}$ by the transmitting antennas. On the user side, the inverse precessing is adopted. The spatial samples of these superimposed signals are obtained by M antennas and are sent into the RF combiner $\mathbf{P} \in \mathbb{C}^{M \times K_r}$ (in which the modulus of each element is a constant, i.e., $1/\sqrt{M}$) and come out after pass through the digital combiner $\mathbf{Q} \in \mathbb{C}^{K_t \times S}$. It should be noted that $S \leq K_t \ll N$ and $M \gg K_r \geq S$. In this study, to apply the SVD method into the digital precoder and combiner, we consider $S = K_t = K_r$.

Assume that the signal vector $\mathbf{s} \in \mathbb{C}^{S \times 1}$ meets $\mathbb{E}[\mathbf{s}\mathbf{s}^H] = \mathbf{I}_S$; then, the outputs of the receiver can be modeled as

$$\hat{\mathbf{s}} = \mathbf{Q}^H \mathbf{P}^H \mathbf{H} \mathbf{V} \mathbf{W} \mathbf{s} + \mathbf{Q}^H \mathbf{P}^H \mathbf{z}, \tag{1}$$

where $(\cdot)^H$ is Hermitian transpose operator and $\mathbf{z} \sim \mathcal{CN}(0, \sigma^2 \mathbf{I}_M)$ denotes additive white Gaussian noise.

Then, the spectrum efficiency R can be written as

$$R = \log_2 \left| \mathbf{I} + \frac{1}{\sigma^2} \mathbf{C}^{-1} \mathbf{Q}^{\mathbf{H}} \mathbf{P}^{\mathbf{H}} \mathbf{H} \mathbf{V} \mathbf{W} \mathbf{W}^{\mathbf{H}} \mathbf{V}^{\mathbf{H}} \mathbf{H}^{\mathbf{H}} \mathbf{P} \mathbf{Q} \right|, \tag{2}$$

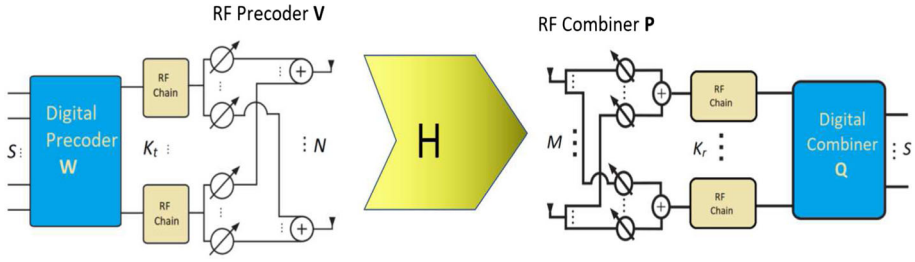

Fig. 1 Block diagram of a P2P MIMO system

where $\mathbf{C} = \mathbf{Q}^H\mathbf{P}^H\mathbf{P}\mathbf{Q}$.

We define the effective channel as

$$\bar{\mathbf{H}} \triangleq \mathbf{P}^H\mathbf{H}\mathbf{V}, \tag{3}$$

and do the singular value decomposition as

$$\bar{\mathbf{H}} = \bar{\mathbf{U}}\boldsymbol{\Lambda}\bar{\mathbf{V}}^H. \tag{4}$$

We set the digital precoder and combiner as

$$\mathbf{Q} = \bar{\mathbf{U}}, \tag{5a}$$

$$\mathbf{W} = \bar{\mathbf{V}}\boldsymbol{\Gamma}^{1/2}, \tag{5b}$$

where $\boldsymbol{\Gamma}^{1/2}$ is dialog matrix of power allocations for each data stream.

It can be further assumed that $\mathbf{C} \approx \mathbf{I}$ [10], and from (5)–(6) the data rate can be rewritten as follows:

$$R = \log_2\left|\mathbf{I} + \frac{1}{\sigma^2}\boldsymbol{\Lambda}^2\boldsymbol{\Gamma}\right| = \sum_{k=1}^{S}\log_2\left(1 + \frac{1}{\sigma^2}\lambda_k^2\gamma_k\right) \tag{6}$$

where $\boldsymbol{\Gamma} = diag(\gamma_1, \ldots, \gamma_S)$.

3 Hybrid Precoder Design

From above, we can see that the task of the hybrid precoding is to find out the RF precoder $\mathbf{V}$, the RF combiner $\mathbf{P}$ and the power allocation matrix $\boldsymbol{\Gamma}$, which can be formulated as follows:

$$\begin{aligned} \max_{\mathbf{V},\mathbf{P},\boldsymbol{\Gamma}} \quad & \sum_{k=1}^{S}\log_2\left(1 + \frac{1}{\sigma^2}\lambda_k^2\gamma_k\right) \\ s.t. \quad & |V_{n,m}| = 1/\sqrt{N}, \forall n, m \\ & |P_{i,j}| = 1/\sqrt{M}, \forall i, j \\ & tr(\mathbf{V}\mathbf{W}\mathbf{W}^H\mathbf{V}^H) \le P_0 \end{aligned} \tag{7}$$

where P_0 is the power budget for the transmitting system.

In the following contents, we will iteratively realized the RF precoding and digital precoding until convergence.

3.1 RF Precoding

First, by fixing $\boldsymbol{\Gamma}$, the RF precoding can be captured by the following optimization problem

$$\begin{aligned} \max_{\mathbf{V},\mathbf{P}} \quad & \sum_{k=1}^{S} \log_2\left(1+\frac{1}{\sigma^2}\lambda_k^2\gamma_k\right) \\ s.t. \quad & |V_{n,m}| = 1/\sqrt{N}, \quad \forall n,m \\ & |P_{i,j}| = 1/\sqrt{M}, \quad \forall i,j \end{aligned} \tag{8}$$

In order to eliminate the constant modulus constraint for each RF precoder element, we define the RF precoder $\mathbf{V}$ and the RF combiner $\mathbf{P}$ as

$$\mathbf{V} \triangleq \mathbf{e}^{\mathbf{iX}}/\sqrt{\mathbf{N}} \tag{9a}$$

$$\mathbf{P} \triangleq \mathbf{e}^{\mathbf{iY}}/\sqrt{\mathbf{M}} \tag{9b}$$

where $\mathbf{X} \in \mathbb{R}^{N\times S}$ and $\mathbf{Y} \in \mathbb{R}^{M\times S}$ is matrices and $i = \sqrt{-1}$. The following work focuses on finding the derivative of R with respect to $\mathbf{X}$ and $\mathbf{Y}$.

We first find the derivative of data rate with respect to $\bar{H}_{ij}$:

$$\begin{aligned} \frac{\partial R}{\partial \bar{H}_{ij}} &= \sum_{k=1}^{S} \frac{\partial \log_2\left(1+\frac{1}{\sigma^2}\lambda_k^2\gamma_k\right)}{\partial \bar{H}_{ij}} \\ &= \frac{2}{\sigma^2 \ln 2}\sum_{k=1}^{S} \frac{1}{1+\lambda_k^2\gamma_k/\sigma^2}\cdot\gamma_k\lambda_k\cdot\frac{\partial\lambda_k}{\partial\bar{H}_{ij}} \\ &= \frac{2}{\sigma^2 \ln 2}\sum_{k=1}^{S} \frac{1}{1+\lambda_k^2\gamma_k/\sigma^2}\cdot\gamma_k\lambda_k\cdot\bar{U}_{ik}^{*}\bar{V}_{jk}. \end{aligned} \tag{10}$$

Then according to the derivative chain rule, we have

$$\begin{aligned} \frac{\partial R}{\partial V_{ij}} &= tr\left[\left(\frac{\partial R}{\partial \bar{\mathbf{H}}}\right)^T \frac{\bar{\mathbf{H}}}{\partial V_{ij}}\right] \\ &= tr\left[\left(\frac{\partial R}{\partial \bar{\mathbf{H}}}\right)^T \mathbf{P}^H\mathbf{H}\mathbf{J}^{ij}\right] \\ &= \left[\left(\frac{\partial R}{\partial \bar{\mathbf{H}}}\right)^T \mathbf{P}^H\mathbf{H}\right]_{ji}, \end{aligned} \tag{11a}$$

$$\begin{aligned} \frac{\partial R}{\partial P_{ji}} &= tr\left[\left(\frac{\partial R}{\partial \bar{\mathbf{H}}}\right)^T \frac{\bar{\mathbf{H}}}{\partial P_{ji}}\right] \\ &= tr\left[\left(\frac{\partial R}{\partial \bar{\mathbf{H}}}\right)^T \mathbf{J}^{\mathbf{ij}}\mathbf{H}\mathbf{V}\right]. \end{aligned} \tag{11b}$$

Thus, we can get

$$\frac{\partial R}{\partial \mathbf{V}} = (\mathbf{P}^H\mathbf{H})^T\frac{\partial R}{\partial \bar{\mathbf{H}}}, \tag{12a}$$

$$\frac{\partial R}{\partial \mathbf{P}} = \mathbf{H}\mathbf{V}\left(\frac{\partial R}{\partial \overline{\mathbf{H}}}\right)^{T}. \tag{12b}$$

Now, we define the directional matrix of $\mathbf{X}$ and $\mathbf{Y}$ as

$$\mathbf{D}^{X} \triangleq \frac{\partial R}{\partial \mathbf{X}} = i\frac{\partial R}{\partial \mathbf{V}} \circ \mathbf{V}, \tag{13a}$$

$$\mathbf{D}^{Y} \triangleq \frac{\partial R}{\partial \mathbf{Y}} = i\frac{\partial R}{\partial \mathbf{P}} \circ \mathbf{P}, \tag{13b}$$

where $\circ$ is Hadamard (elementwise) product.

The RF precoder and combiner can be updated through their directional matrices respectively. To ensure that the updated $\mathbf{X}$ and $\mathbf{Y}$ will always be real matrices, we only take the real part of the directional matrices. Besides, we normalize the directional matrix by its 2-norm value. Then, the update equation for the variable matrix can be formulated as follows

$$\mathbf{X}_{t+1} = \mathbf{X}_t + \delta_X \frac{\Re\left(\mathbf{D}_t^{\mathfrak{X}}\right)}{||\mathbf{D}_t^{X}||}, \tag{14a}$$

$$\mathbf{Y}_{t+1} = \mathbf{Y}_t + \delta_Y \frac{\Re\left(\mathbf{D}_t^{\mathfrak{Y}}\right)}{||\mathbf{D}_t^{Y}||}, \tag{14b}$$

where δ_X and δ_Y are Armijo step sizes for $\mathbf{X}$ and $\mathbf{Y}$ respectively, and t is the iteration time.

The initialization of $\mathbf{X}_0$ and $\mathbf{Y}_0$ can be random real matrices; the update can be stopped when the iteration time is greater than the threshold time, or when the 2-norm of the directional matrices are small enough. These conditions can be expressed as (15a) or (15b), respectively:

$$t > T_{threshold}, \tag{15a}$$

$$\max\left\{||\mathbf{D}_t^{X}||_F^2, \mathbf{D}_t^{Y}||_F^2\right\} < \varepsilon. \tag{15b}$$

3.2 Digital Precoding

After obtain the RF precoder and combiner, from (5) we can see that the only remaining work for obtaining the digital precoder and combiner is to capture the power allocation matrix $\boldsymbol{\Gamma}$, and it can be expressed as follows:

$$\begin{aligned} \max_{\boldsymbol{\Gamma}} \quad & \sum_{k=1}^{S} \log_2\left(1 + \frac{1}{\sigma^2}\lambda_k^2\gamma_k\right) \\ s.t. \quad & tr(\mathbf{V}\mathbf{W}\mathbf{W}^H\mathbf{V}^H) \le P_0, \end{aligned} \tag{16}$$

which can be easily solved by the well-known waterfilling method [6].

4 Simulation

In this section, in order to examine the performance of the proposed algorithm, we compared the proposed algorithm with the Algorithms in [3, 10] and the fully digital precoding under two different channel models, i.e., mmWave channel model and Rayleigh fading channel model. Besides, to evaluate the efficiency of the proposed algorithm, computational complexities of proposed algorithm and the Algorithms in [3, 10] were analyzed. What is more, in practical implementation, the phase array in RF precoding is tend to be quantized. Hence, we also studied the performances of the proposed algorithm with 1-bit and 2-bit quantized phase-shifter array. At last, the convergence rate of the proposed algorithm was analyzed.

4.1 MmWave Channel

In this subsection, we simulated the proposed algorithm and the Algorithms in [3, 10] and the fully digital precoding schema under mmWave channel. The mmWave channel between the BS and the user is modeled as a geometric channel with L paths [3], which can be formulated as follows:

$$\mathbf{H} = \sqrt{\frac{MN}{L}} \sum_{l=1}^{L} \alpha_l \mathbf{a}_r(\phi_l) \mathbf{a}_t(\psi_l)^H, \tag{17}$$

where $\alpha_l \sim \mathcal{CN}(0,1)$ is the complex gain of the lth path between the BS and the user, $\phi_l \in [0, 2\pi)$ and $\psi_l \in [0, 2\pi)$ are directions of arrival (DOA) of the transmitter and the receiver respectively and $\mathbf{a}_r(\cdot)$ and $\mathbf{a}_t(\cdot)$ are antenna array response vectors on the BS and the user sides, respectively. For the uniform linear array with N antenna elements, we have

$$\mathbf{a}(\theta) = \frac{1}{\sqrt{N}} [1, e^{ik_0 d \sin(\theta)}, \ldots, e^{ik_0 d(N-1)\sin(\theta)}]^T, \tag{18}$$

where k_0 is the wave number and d is the antenna spacing.

To study the performances of the proposed algorithm under different antenna configurations, we compared the performances of the proposed method with those of the existing schemes under two different antenna configurations, i.e., $(M, N) = (16, 128), (64, 128)$. Besides, we set the number of data stream as $S = 8$, and the number of the multipath as $L = 32$. The results are shown in Fig. 2.

Figure 2 shows that the performances of the proposed algorithm and the Algorithm in [10] can match that of the fully digital precoding under different antenna configurations. By comparing Fig. 2a, b, we can see the performance of the Algorithm in [3] becomes closer to that of the fully digital precoding, this is because the channel become relative spare as antenna number increases.

To further investigate the relationships between the performances of these algorithms and the the sparsity of the mmWave channel, we calculated the average spectrum efficiencies versus the number of multipath L through 30 times simulations. In this experiment, we still set the the data stream number as $S = 8$, the antenna configuration as $(M, N) = (64, 128)$, and the SNR = 0 dB. The results are shown in Fig. 3.

Figure 3 demonstrates that the performances of these algorithms are monotonic increasing when the path number is smaller than a certain value, i.e., $L = 16$; Whlie these performances begin to decline when the path number exceed $L = 16$. Because the

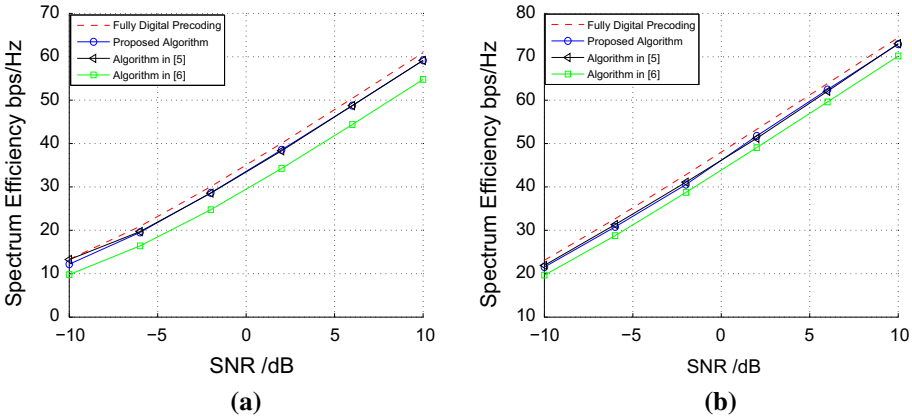

Fig. 2 Spectrum efficiencies under different antenna configurations. **a** $(M, N) = (16, 128)$. **b** $(M, N) = (64, 128)$

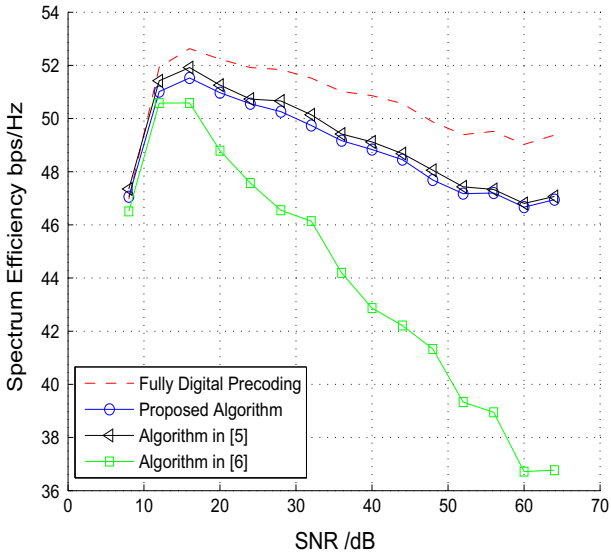

Fig. 3 Spectrum efficiencies under different numbers of multipath

Algorithm in [3] is sensitive to channel sparsity, its performance becomes rapidly deteriorated. This indicates that the proposed algorithm is robust in the multipath mmWave channel model.

4.2 Rayleigh Fading Channel

In this subsection, the propagation environment between the BS and the MSs is modeled as a Rayleigh channel, in which each element of $\mathbf{H}$ is an independent and identically distributed (i.i.d) complex Gaussian random variable. It is known that the mmWave channel can be approximated to Rayleigh channel as the path number limits to infinity. Hence, we set the path number as $L = 256$. The transmitting antenna number is 128, and the receiving

antenna number is 16. Also, the data stream number is 8. The performance of the proposed method is examined under the SNR from -10 to 10 dB. The results are shown in Fig. 4.

Figure 4 demonstrates that the performances of the proposed method and the Algorithm in [10] are almost the same and match to that of the fully digital precoding, while the Algorithm in [3] can not adapt to Rayleigh fading channel for the reason that this channel is not sparse, i.e., the path number L is too large compare to transmitting/receiving antennas number. This simulation shows that the performance of the proposed method matches the results in Fig. 3.

4.3 Complexity Analysis

Assume that arithmetic with individual elements has complexity $\mathcal{O}(1)$, and we ignore the operations of addition and subtraction. The computational complexity of the matrix multiplication with one $n \times m$ matrix and one $m \times p$ matrix is $\mathcal{O}(nmp)$; the computational complexity of the SVD for a $m \times n$ matrix $(m \leq n)$ is $\mathcal{O}(mn^2)$ and the computational complexity of the $n \times n$ matrix inversion is $\mathcal{O}(n^3)$ (assume we adopt the Gauss-Jordan elimination method). For the reason that the procedures of obtaining the RF precoder and RF combiner are nearly the same, we here only calculate the computational complexity of RF precoder. Besides, we assume $S \ll \min\{M, N\}$. The comparisons of computational complexity of RF precoder between the proposed algorithm and the Algorithms in [3, 10] are shown in Table 1.

Table 1 clearly shows that the computational complexity of the Algorithm in [10] is at least S times higher than the proposed algorithm, while the performances of these algorithms are nearly the same. Thus, the efficiency of the proposed algorithm is at least S times higher than that of the Algorithm in [10]. Because $S \ll \min\{M, N\}$ and $L \ll \min\{M, N\}$ when the channel is sparse, the computational complexity in [3] is possible to be lower than that of the proposed algorithm. However, Figs. 2, 3, 4 and 5 show that the performance of the proposed algorithm is much better than that of the Algorithm in [3].

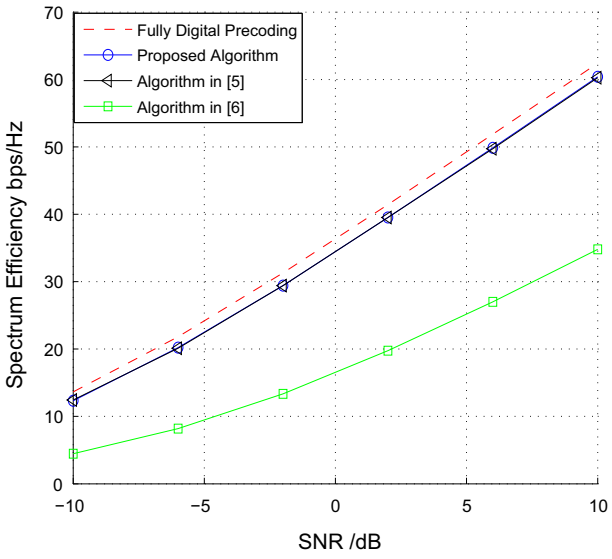

Fig. 4 Performances of different hybrid precoders in Rayleigh fading channel

Table 1 Computational analysis

Algorithms	Computational complexities
Proposed algorithm	$\mathcal{O}(2SMN + 2S^2N)$
Algorithm in [10]	$\mathcal{O}(3S^2N^2 + 2S^3N)$
Algorithm in [3]	$\mathcal{O}(S^2LN + S^2L^2 + 2S^3N)$

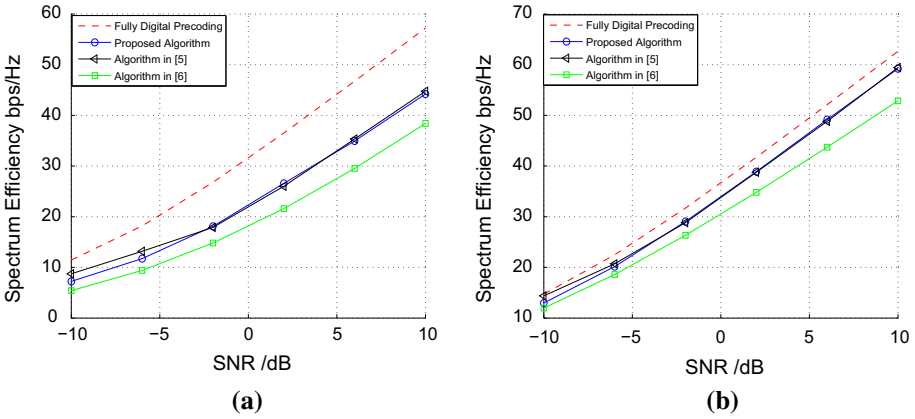

Fig. 5 The impact of quantized phases on the sum spectral efficiency. **a** 1-bit phase-shifter array. **b** 2-bit phase-shifter array

4.4 Quantized Phase-Shifter Array

In practical implementation, the phase of each element in the RF precoder tends to be quantized. Hence, it is necessary to research the performance of the proposed RF precoder in this realistic scenario. The phase for each entry in the RF precoder $\mathbf{V}$ can be selected by the following equation:

$$\hat{\phi} = \arg\min_{\phi_n} |\phi - \phi_n|, \quad n \in [0, 1, \ldots, 2^B - 1] \tag{19}$$

where ϕ is the analog phase, B is a positive integer and $\phi_n = 2\pi n/2^B$.

In this experiment, we still consider the mmWave channel and set the path number as $L = 16$. The transmitting antennas number is 128, the receiving antennas number is 16 and the data stream is 8. The performances of the hybrid precoding schemas with 1-bit and 2-bit quantized phase-shifter array are shown in Fig. 5.

Figure 5 demonstrate that, under both 1-bit and 2-bit phase-shifters, the sum spectral efficiency of the proposed scheme and the Algorithm in [10] are very closed to each other and much better than that of the Algorithm in [3]. Especially, the spectral efficiency of the proposed algorithm and the Algorithm in [10] under a 2-bit phase-shifter match the performance of the fully digital precoding. This confirms that the proposed algorithm is very robust in practical scenarios.

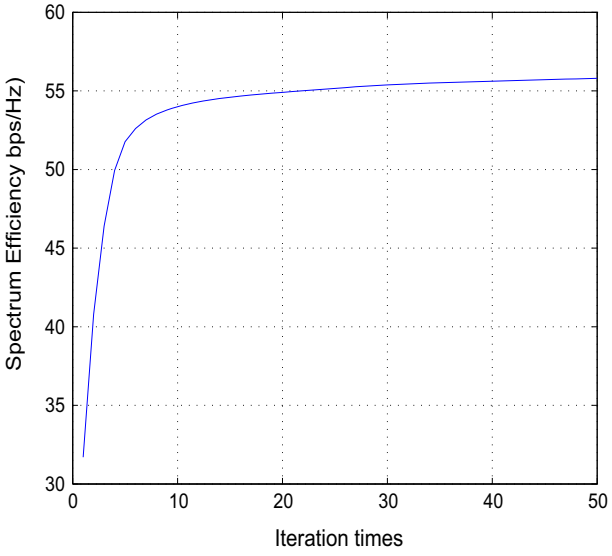

Fig. 6 Convergence rate of the spectrum efficiency

4.5 Convergence Analysis

In this subsection, we examine the convergence rate of the proposed algorithm. We considered the channel model between BS and the user as Rayleigh fading channel. Besides, we set the antenna configuration of $(M, N) = (16, 128)$, the SNR $= 0$ dB, $T_{threshold} = 50$ and $\varepsilon = 0.1$. The spectrum efficiency and 2-norm of the directional matrices of $||\mathbf{D}_t^X||_F^2$ and $||\mathbf{D}_t^Y||_F^2$ versus iteration times are shown in Figs. 6 and 7, respectively.

Figure 6 shows that the spectrum efficiency of the proposed algorithm begins to become stable at about the 20th step and Fig. 7 demonstrates that the 2-norm of directional matrices of the RF precoder and RF combiner reach convergence at about the 20th step.

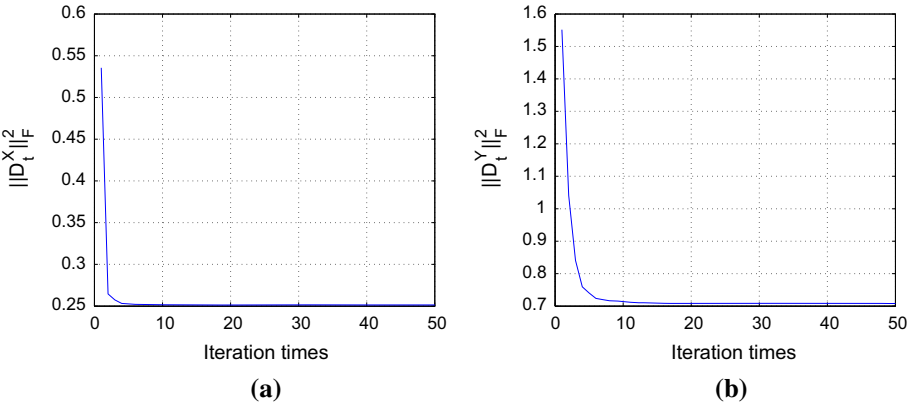

Fig. 7 Convergence rate of the directional matrices of RF precoder and combiner. **a** Convergence rate of the RF precoder. **b** Convergence rate of the RF combiner

The results of Figs. 6 and 7 match each other. Hence, the Fig. 7 can be an index of the convergence. These results confirm that the convergence rate of the proposed algorithm is fast.

5 Conclusion

This paper considered a hybrid analog and digital precoding for single user MIMO communication system and proposed an innovative matrix adaptive gradient descent algorithm to design the RF precoder and combiner, and employed the SVD method and waterfilling method to design the digital precoder and combiner. The proposed algorithm provides a sub-optimal solution. The performance of the proposed algorithm approximates and even exceeds that of the existing algorithms with a far lower computational complexity. The good performance of the proposed algorithm with the quantized phase-shifter array shows that it is greatly robust. Hence, it can be considered as a candidate of the hybrid precoding scheme.

References

1. Alkhateeb, A., El Ayach, O., Leus, G., & Heath, R.W. (2013). Hybrid precoding for millimeter wave cellular systems with partial channel knowledge. In Information Theory and Applications Workshop (ITA) (pp. 1–5). IEEE.
2. Andrews, J. G., Buzzi, S., Choi, W., Hanly, S. V., Lozano, A., Soong, A. C. K., et al. (2014). What will 5g be? *IEEE Journal on Selected Areas in Communications*, *32*(6), 1065–1082. https://doi.org/10.1109/jsac.2014.2328098.
3. El Ayach, O., Rajagopal, S., Abu-Surra, S., Pi, Z., & Heath, Robert W. (2014). Spatially sparse precoding in millimeter wave mimo systems. *IEEE Transactions on Wireless Communications*, *13*(3), 1499–1513. https://doi.org/10.1109/twc.2014.011714.130846.
4. Gao, X., Dai, L., Han, S., Chin-Lin, I., & Heath, R. W. (2016). Energy-efficient hybrid analog and digital precoding for mmwave mimo systems with large antenna arrays. *IEEE Journal on Selected Areas in Communications*, *34*(4), 998–1009. https://doi.org/10.1109/jsac.2016.2549418.
5. Hoydis, J., ten Brink, S., & Debbah, M. (2013). Massive mimo in the UL/DL of cellular networks: How many antennas do we need? *IEEE Journal on Selected Areas in Communications*, *31*(2), 160–171. https://doi.org/10.1109/jsac.2013.130205.
6. Jindal, N., Rhee, W., Vishwanath, S., Jafar, S. A., & Goldsmith, A. (2005). Sum power iterative waterfilling for multi-antenna gaussian broadcast channels. *IEEE Transactions on Information Theory*, *51*(4), 1570–1580. https://doi.org/10.1109/tit.2005.844082.
7. Larsson, E. G., Edfors, O., Tufvesson, F., & Marzetta, T. L. (2014). Massive mimo for next generation wireless systems. *IEEE Communications Magazine*, *52*(2), 186–195.
8. Lee, J., & Lee, Y.H. Af relaying for millimeter wave communication systems with hybrid rf/baseband mimo processing. In IEEE International Conference on Communications (ICC), 2014 (pp. 5838–5842). IEEE.
9. Lee, Y. Y., Wang, C. H., & Huang, Y. H. (2015). A hybrid RF/baseband precoding processor based on parallel-index-selection matrix-inversion-bypass simultaneous orthogonal matching pursuit for millimeter wave mimo systems. *IEEE Transactions on Signal Processing*, *63*(2), 305–317. https://doi.org/10.1109/tsp.2014.2370947.
10. Sohrabi, F., & Yu, W. (2016). Hybrid digital and analog beamforming design for large-scale antenna arrays. *IEEE Journal of Selected Topics in Signal Processing*, *10*(3), 501–513. https://doi.org/10.1109/jstsp.2016.2520912.

Yongpan Feng received the B.E. degree in computer and electronics engineering from Henan Normal University, Xinxiang, Henan, China, and the M.A.Sc degree in electrical engineering from the Nanjing University of Information Science and Technology (NUIST), Nanjing, China, in 2011 and 2014, respectively. Additional, he won the outstanding master's Thesis Award from NUIST in June, 2014. He is currently pursuing the Ph.D. degree in electrical engineering at the Pusan National University (PNU), Busan, Korea. His research interests include millimeter wave communication, signal processing, compressive sensing, mathematical optimization and machine learning.

Suk Chan Kim (S'95-M'00-SM'05) received the B.S.E. (summa cum laude) degree in electronics engineering from Pusan National University (PNU), Busan, Korea, in February 1993 and the M.S.E. and Ph.D. degrees in electrical engineering from the Korea Advanced Institute of Science and Technology (KAIST), Daejeon, Korea, in February 1995 and 2000, respectively. He was a Postdoctoral Researcher with the Electronics and Telecommunications Research Institute (ETRI), Princeton University, Princeton, NJ, and Lehigh University, Bethlehem, PA, in 2000 and 2001, respectively. He is currently an Professor with the Department of Electronics Engineering and has been a Researcher with the Research Institute of Computer Information and Communication (RICIC), PNU, since 2002. His current research interests include mobile communications and statistical signal processing. Dr. Kim is a member of the Institute of Electronics Engineers of Korea (IEEK) and the Korean Institute of Communication Sciences (KICS). He won a scholarship from the Hyundai Asan Foundation in 1992, a Grant for Young Scientists from the Korea Research Foundation (KRF) in 1993, a Grant for Postdoctoral Study Abroad from the Korea Science and Engineering Foundation (KOSEF) in 2000, and a Haedong Paper Award from KICS in 2005.